HETEROCYCLES, Vol. 91, No. 8, 2015, pp. 1603 - 1613. © 2015 The Japan Institute of Heterocyclic Chemistry
Received, 28th May, 2015, Accepted, 29th June, 2015, Published online, 8th July, 2015
DOI: 10.3987/COM-15-13258

CRYSTAL STRUCTURES OF 2-FURYLBENZIMIDAZOLES WITH ANTIANGIOGENIC INHIBITION OF VEGF IN CELL LINE MCF-7

Keith J. Flanagan,[a] Yasser M. Shaker,[b] Ahmed Temirak,[b] Hoda I. El Diwani,[b] and Mathias O. Senge[c]*

[a] School of Chemistry, SFI Tetrapyrrole Laboratory, Trinity Biomedical Sciences Institute, 152-160 Pearse Street, Trinity College Dublin, The University of Dublin, Dublin 2, Ireland

[b] Division of Pharmaceutical and Drug Industries, Department of Chemistry of Natural and Microbial Products, National Research Centre, Dokki, Cairo, 12622, Egypt

[c] Medicinal Chemistry, Institute of Molecular Medicine, Trinity Centre for Health Sciences, Trinity College Dublin, St. James's Hospital, Dublin 8, Ireland. E-mail: sengem@tcd.ie

Abstract – The first crystal structures of four 2-furylbenzimidazole acetohydrazide derivatives are reported herein. The compounds have been shown to be planar with a small cant that varies from 4 to 30°. The X-ray crystal structure of the compounds **7**-**10** revealed that compounds are oriented in the *cis* configuration which suggests that the acid hydrazide group is essential for the enhanced potency of 2-furylbenzimidazoles as anti-angiogenic agents.

INTRODUCTION

2-Furylbenzimidazoles have a variety of interesting pharmacological characteristics which include the use as anti-viral agents and chemotherapeutics for anti-cancer.[1,2] They have also found application as anti-histamines, anti-ulcer and fungicidal therapeutics.[3] Benzimidazoles and their derivatives have an established ability to bind and intercalate to DNA.[4] The bis-benzimidazole drug Hoechst 33258 **1** has been widely used as a fluorescent DNA stain and is well known to bind in the minor-groove of B-DNA.[5] 2-Phenylbenzimidazole have been found to intercalate between base pairs of DNA by Kubota *et al.* and Nakano *et al.*[6,7] There are many examples in the literature of 2-substituted benzimidazoles as potent inhibitors in angiogenesis through the targeting of the vascular endothelial growth factor (VEGF), such as

Dovitinib **2**, which exhibits efficacy in renal cell carcinoma and Albendazole **3**, a widely used drug for hydatid disease, shows an anti-angiogenesis effect in non-cancerous models of angiogenesis.[8-10] Li *et al.* demonstrated that a tetra cationic heterocycle containing a phenyl furanylbenzimidazole (DB340) **4** shows increased selectivity towards REE RNA stem loops.[11] 2-Furylbenzimidazoles have gained a particular interest, as furan rings also exhibit DNA intercalating abilities.[12] Patel *et al.* have shown the model inhibitor based benzimidazole compounds docking within the receptor site of the hepatitis C virus through π-π and C-H-π interactions.[13] Even though aromatic interactions play major roles, in organic reaction and further more biological systems, as both these reaction are common in 2-furylbenzimidazoles, there is very little literature with regards to structural determination of optimum geometries of these compounds. In 2007 Hranjec *et al.* published the X-ray structure of an 2-(1*H*-benzimidazol-2-yl)-3-(4-*N*,*N*-dimethylaminophenyl)-acrylonitrile hydrochloride monohydrate **5** (Figure 1) and subsequent fluorimetric titration with ct-DNA.[14] Geiger *et al.* published work using X-ray diffraction on benzimidazole substituted compounds which participate in a 'head to tail' arrangement due to intramolecular C-H-π interactions 2-(furan-2-yl) and 1-(furan-2-ylmethyl) **6** and π-π interactions involving the furan substituents between inversion centers related molecules.[15] We report herein the structures of the compounds *N*'-(4-methoxybenzylidene)-2-(2-furan-2-yl)-1*H*-benzo[*d*]imidazol-1-yl)acetohydrazide **7**, 2-(2-(furan-2-yl)-1*H*-benzo[*d*]imidazol-1-yl)-*N*'-(1-phenylethylidene)acetohydrazide **8**, 2-(2-(furan-2-yl)-1*H*-benzo[*d*]imidazol-1-yl)-*N*''-(1-*p*-tolylethylidene)acetohydrazide **9** and 2-[2-(furan-2-yl)-1*H*-1,3-benzodiazol-1-yl]-*N*'-[(1*Z*)-(4-methylphenyl)methylidene]acetohydrazide **10** for the purpose of establishing a relationship between structure and potency of inhibition.

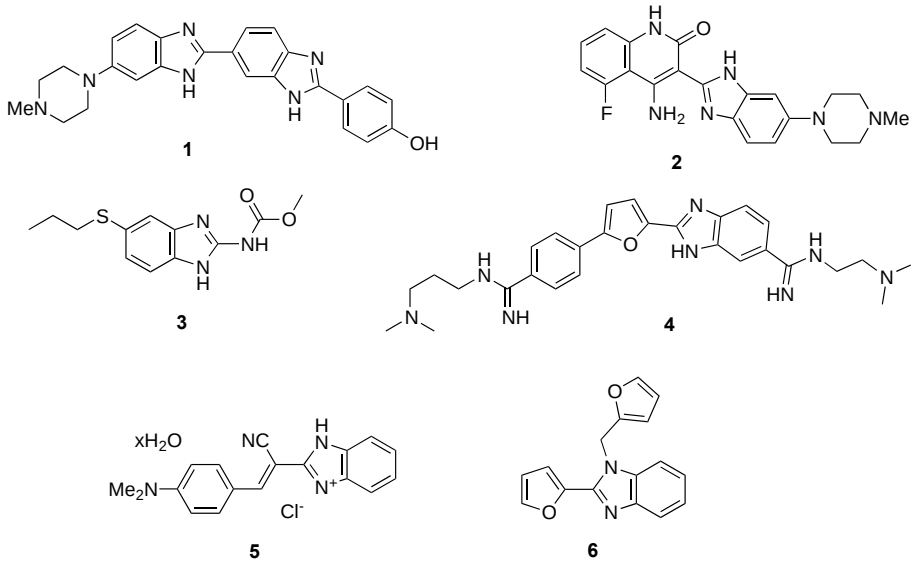

Figure 1. Hoechst 33258 **(1)**, Dovitinib **(2)**, Albendazole **(3)**, DB340 **(4)**, 2-(1*H*-benzimidazol-2-yl)-3-(4-*N*,*N*-dimethylaminophenyl)-acrylonitrile hydrochloride monohydrate **(5)**, 2-(furan-2-yl)-1-(furan-2-ylmethyl)-1*H*-benzo[*d*]imidazole **(6)**

RESULTS AND DISCUSSION

Tumor-induced angiogenesis plays a crucial role in progression and supporting tumor growth by allowing metastatic tumor cells to enter circulation and providing blood supply. The 2-furylbenzimidazoles showed remarkable anti-angiogenic activity through targeting the vascular endothelial growth factor receptor (VEGFR2).[2,16-20] Substitution on position 1 of the 2-furylbenzimidazole moiety with acid hydrazide groups as in compounds **7-10** significantly enhanced the antiangiogenic properties of the 2-furylbenzimidazoles.[2] Furthermore, molecular modelling studies proposed that the acid hydrazide moiety in its *cis* configuration is stabilizing the compound in the active site of the VEGFR2 through the stabilization with two hydrogen bonds with ASP1046 and GLU885 amino acids.[2]

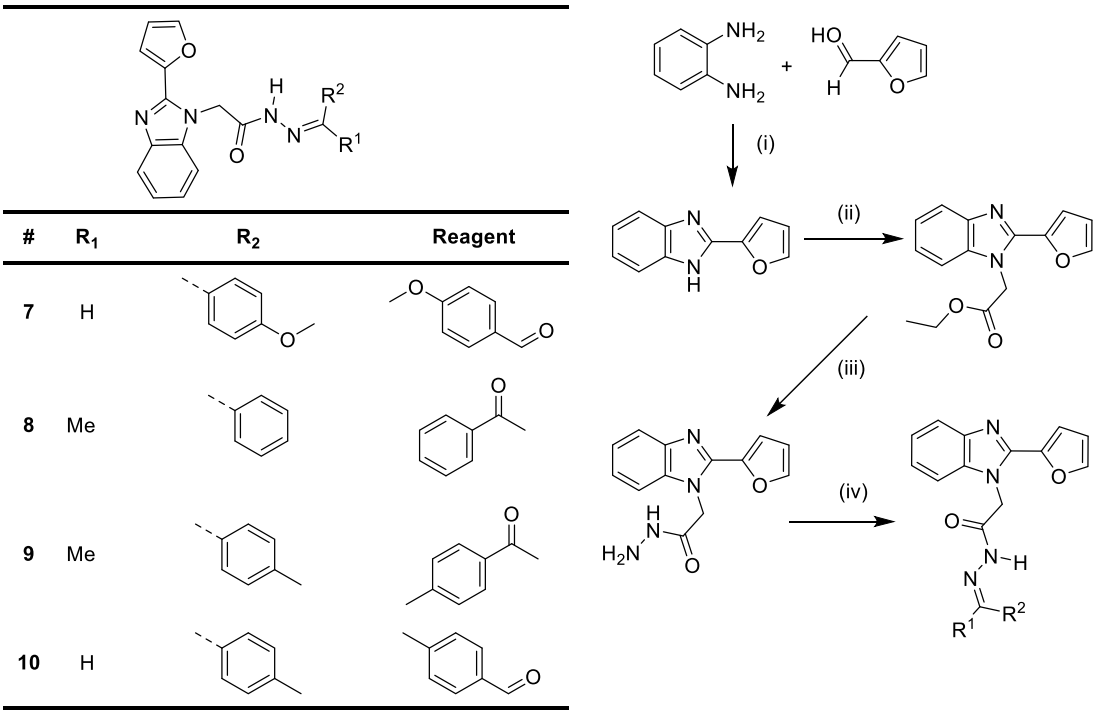

Figure 2. 2-Furylbenzimidazole derivatives **7-10** synthetic pathway: (i) *p*-toluenesulfonic acid, DMF, 100 °C; (ii) ethyl 2-bromoacetate, K_2CO_3, acetone, RT; (iii) hydrazine hydrate, EtOH, 90 °C; (iv) aryl aldehydes or ketones, EtOH/AcOH acid (24:1), reflux

We attempted to crystallization of various derivatives, four of which yielded crystals of sufficient quality for X-ray crystallographic investigations. Indeed, the X-ray crystal structure of the compounds **7-10** in the crystal lattice reported here revealed that compounds are oriented in the *cis* configuration (Figure 3). This may indicate that the acid hydrazide moiety is essential in enhancing the potency of 2-furylbenzimidazoles as anti-angiogenic agents. Within the set of four structures investigated, compounds **7** (R^1 = H, R^2 = *para* methoxyphenyl) and **9** (R^1 = Me, R^2 = *para* methylphenyl) showed the most promising inhibitory activity.[2]

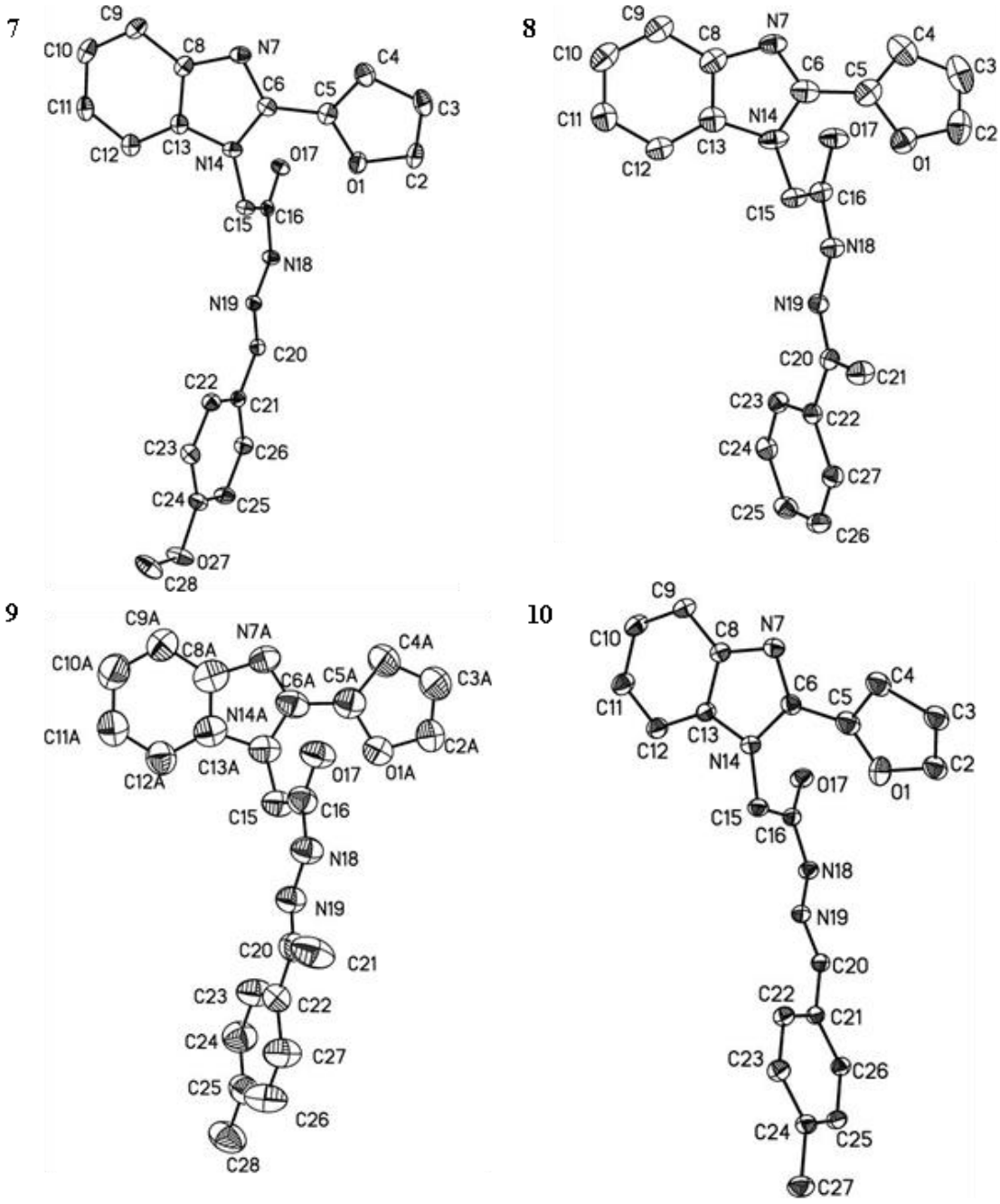

Figure 3. Molecular structure of compounds **7-10** (thermal displacement 50%). Hydrogens and disorder have been omitted for clarity.

Compounds **7-10** were synthesized as reported by Temirak *et al.* using a condensation of the acid hydrazide with selected aldehydes and methyl aryl ketone using an ethanol/acetic acid (24:1) mixture.[2,21] The 2-furylbenzimidazoles **7** and **10** were obtained by slow evaporation in DMSO and **8** and **9** were obtained from liquid diffusion from 1,4-dioxane/*n*-hexane. The compounds crystallized quickly giving crystals suitable for analysis within a week. The molecular structures of the individual compounds are shown in Figure 2. The structures are defined by a furan ring joined to a benzimidazole ring over a single bond. The 2-furylbenzimidazole part is almost planar with a small but noticeable cant that varies from

structure to structure. Overall, the basic structural parameters such as bond length, angles and tilt in the 2-furylbenzimidazoles are comparable to related structures. Selected structural parameters are compiled in Table 1. The substitution of an acetohydrazide chain on the N19 position of each of these compounds varies in the substitution at R^1 and R^2. The acetohydrazide chain is canted between 89-73° from the benzimidazole plane which suggest a minor degree of positional rotational freedom.

Table 1. Selected structural and geometrical parameters of the structures

Compound	**7**	**8**	**9**	**10**
Bond lengths, Å				
C5-C6	1.441(2)	1.432(4)	1.444(8)	1.488(4)
N14-C15	1.4441(19)	1.437(3)	1.426(8)	1.4422(10)
N18-N19	1.3789(17)	1.379(2)	1.379(2)	1.3802(9)
Bond angles, deg.				
N19-C20-H20 (C21)	120.1	125.73(18)	123.2(2)	119.6
C6-N14-C15	130.55(13)	131.1(2)	136.0(7)	127.30(7)
C5-C6-N14	123.19(13)	121.1(2)	123.3(6)	120.2(9)
N14-C6-N7	113.89(14)	115.2(2)	116.3(5)	113.26(7)
Furan/Benzimidazole	11.665	4.753	6.4	29.155
Benzimidazole/side chain	80.156	73.605	77.335	88.8987
Benzimidazole overlap, *Å*	3.23	3.305	2.911	3.409

The tilt of the furan/benzimidazole rings vary from 4-30° which indicates a larger rotational freedom is present in this part of the molecule which shows that the compounds studied have mobility to achieve optimum conformation within a binding pocket. This tilt has also been reported in previous crystal structures by Geiger *et al*.[15] Modelling of the VEGFR2 receptor (PDB entry 3EWH) was carried out by Temirak *et al*.[2] The inhibitory potency of compounds **7-10** has been attributed to the presence of the acetohydrazide chain, which is common in all the compounds and can act as a hydrophilic anchor within a rather hydrophobic binding cleft.[2] The acetohydrazide side chain is able to stabilize the compounds in the binding site toward an aspartic acid group present in the receptor. This is established through a hydrogen bond donor of the N18 proton which is present in the in the crystal structure (Figure 4). The presence of a possible hydrogen bond acceptor (O17) shown in compounds **8-10** (Figure 5) indicates a further stabilizing through hydrogen bonding.

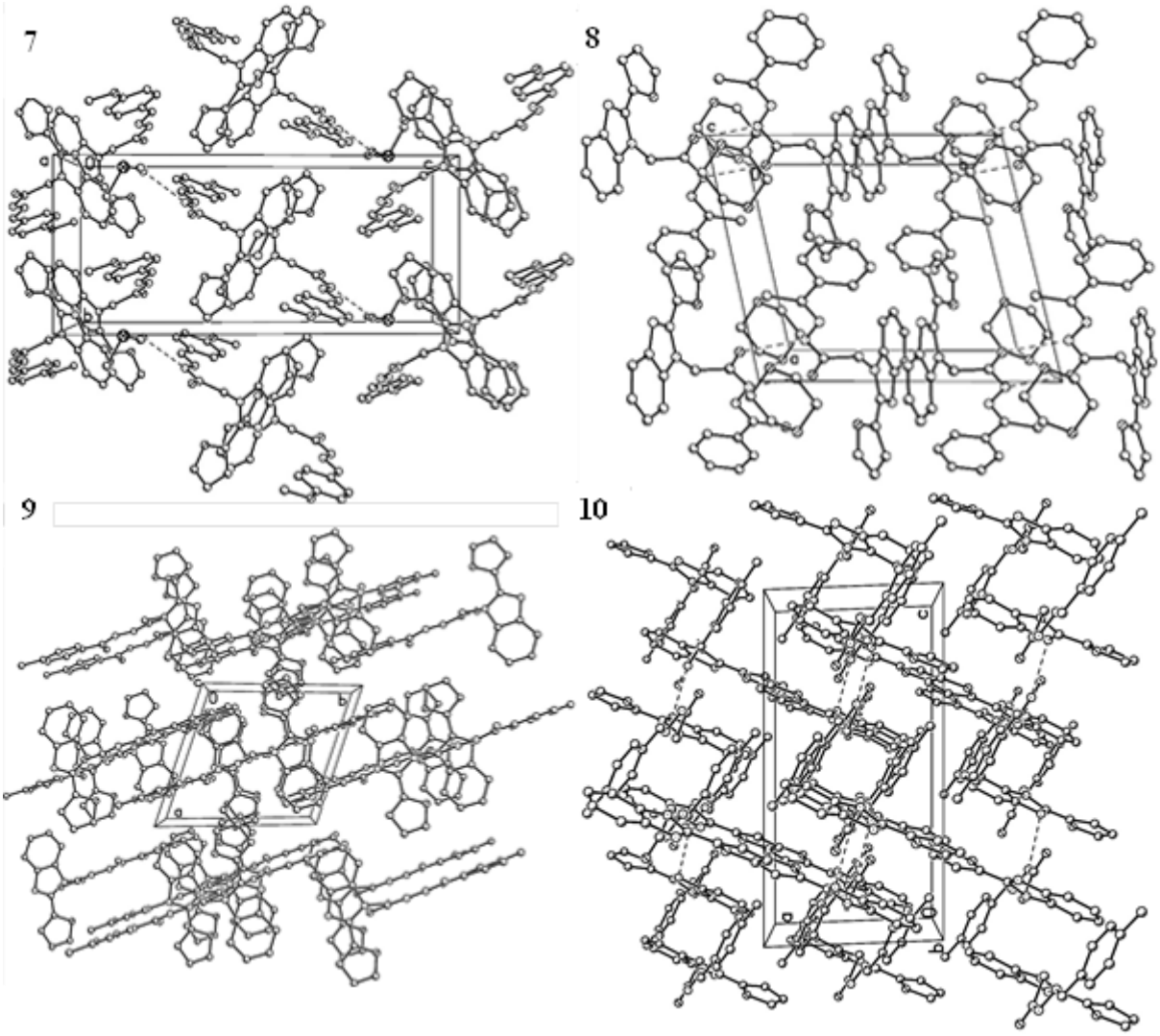

Figure 4. Packing of compounds **7-10** shown with labels omitted. Hydrogen atoms and disordered groups omitted for clarity.

The presence of a double bond in *cis* conformation is considered to be of high importance for the orientation of the inhibitor in the enzyme pocket. The phenyl ring is stabilized by the leucine and isoleucine residues while the benzimidazole ring interacts with the valine and tyrosine residues within the receptor pocket. Temirak *et al.* suggested that a hydrophobic area was covered by the furan ring of the inhibitor. The lack of a suitable hydrogen bond donor to the furan ring suggests that hydrophobic interactions are favorable in this part of the molecule. However, the presence of short contact or pseudo hydrogen bonds as a result of the crystal packing of compound **7** suggests there may be further interaction with residues within the receptor. As the pocket is considered to be highly hydrophobic, lipophilic features either on the phenyl or furyl rings are crucial for good binding and therefore for the activity. This is clearly the case for compounds **9-10** which present a *p*-methyl substitution on the phenyl ring, and with **7**, with a *p*-methoxy substitution. This would also have the additional benefit of reducing oxidation by *p*-hydroxylation with cytochrome p450 *in vivo*. The presence of a methyl group on the acetohydrazide

chain for compounds **8-9** (C21) contributes to the hydrophobic nature of the molecule by increasing lipophilicity. However, weak interaction of this methyl group in the crystal packing with an opposing O17 show a degree of non-classical hydrogen bonding between the protons of C21 and O17. The packing of compounds **7-10** are due to the same classical 'head' (2-furylbenzimidazole) to 'tail' (acetohydrazide side chain) reported by Geiger *et al*.[15] This is facilitated in the hydrogen bonding present in each crystal structure between the N18 proton and O17 **8-9**. There is also a degree of stacking between the 2-furylbenzimidazole rings in the moiety structure. Compounds **7-10** exhibit a staggered head-to-tail overlap with a separation of 3.23, 3.305, 2.911 and 3.409 Å between benzimidazole rings, respectively.

Table 2. List of hydrogen bonding interactions in the crystal structures (Å, deg)

#	D-H···A	D-H	H···A	D···A	D-H··· A2	Symmetry code
7	C2-H2-O1S	0.95	2.56	3.377(2)	144.6	*-x+1/2,y-1/2,-z+3/2*
	C3-H3-O17	0.95	2.53	3.468(2)	167.5	*x,y-1,z*
	C9-H9-O1S	0.95	2.63	3.498(2)	151.5	*-x,-y+1,-z+1*
	C15-H15B-O1	0.99	2.4	2.9404(2)	113.8	*-x,-y+1,-z+1*
	N18-H18-O1S	0.90	1.89	2.7717(1)	169	*-x+1/2,y+1/2,-z+3/2*
8	C15B-H15B-O1B	0.99	2.42	2.918(3)	110.7	–
	N18B-H18B-O17B	0.88	2.01	2.865(2)	162.8	*-x+2,-y,-z+1*
	C21B-H21F-O17B	0.98	2.55	3.185(3)	122.4	*-x+2,-y,-z+1*
	C21B-H21F-O30	0.98	2.58	3.296(3)	130	*-x+2,-y+1,-z+1*
	N18-H18-O17	0.88	1.95	2.801(2)	162.7	*-x+1,-y+1,-z+2*
9	N18-H18A-O17	0.90	1.97	2.860(3)	173	*-x,-y+1,-z+1*
	C3B-H3BA-N7B	0.95	2.6	3.435(2)	146.9	*-x+1,-y+1,-z*
10	C3B-H3BA-O17	0.95	2.62	3.254(2)	124.3	*x+1,y,z*
	C2C-H2CA-O17	0.95	2.46	3.218(9)	136.6	*x+1,y,z*
	C4C-H4CA-O17	0.95	2.46	3.207(11)	135	–
	C4C-H4CA-N18	0.95	2.58	3.515(10)	168.9	–
	N18-H18A-N7	0.9	2.043	2.9173(10)	163.6	*x+1,y,z*

The presence of molecules of solvation, DMSO in **7** and 1,4-dioxane **8**, within a solvent accessible void is facilitated by a loose packing in the crystal structure. In compounds **9-10** solvent molecules are not present in the asymmetric unit and a tighter packing is observed. The absence of a methyl group at the C20 position in compound **10** eliminates interactions with the O17 position which then establishes hydrogen bonding between the N18 proton and the N7 of the benzimidazole ring resulting in a more staggered approach to the overlay of the 2-furylbenzimidazole rings in the crystal packing. Figure 4 show the crystal packing of each compound. Compound **7** exhibits a hydrogen bond between N18 proton and that of the solvent DMSO. As shown in Table 2 there is a short contact present between the O1 of the furan ring and the C15 proton, as well as the C3 proton and the O17 of the acetohydrazide chain. Both

compounds **8** and **9** (R^1 = Me) display hydrogen bonding involving the N18 hydrogen atom and the O17 atom as well as a short contact between C21 and O17 atoms. Compound **10** shows hydrogen bonding between the N18 hydrogen atom and the N7 in the benzimidazole ring.

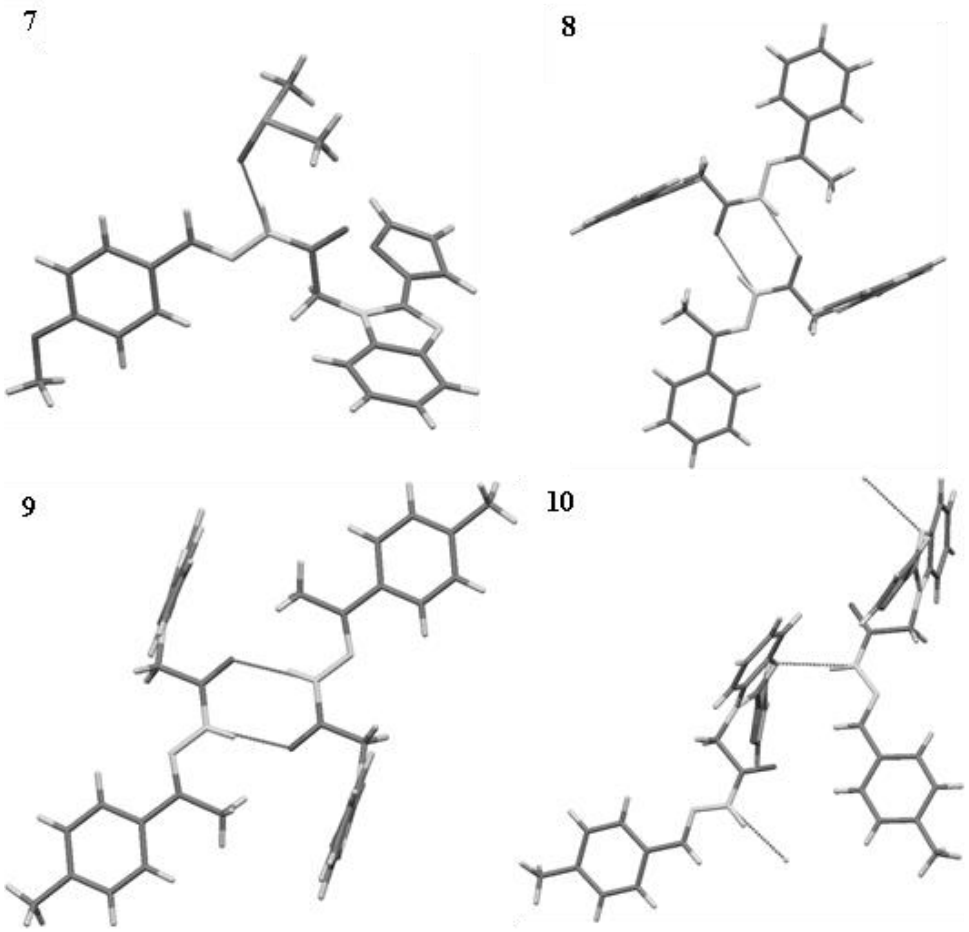

Figure 5. View of hydrogen bonding in compound. Lines indicate hydrogen bonding pattern in the compounds studied.

CONCLUSIONS

In summary, we have reported the first crystal structures of four 2-furylbenzimidazole acetohydrazide derivatives **7-10**. The compounds are planar with a small cant which varies from 4-30°. The acetohydrazide side chain is tilted between 89-73° from the benzimidazole plane, suggesting a minor degree of rotational freedom. The acetohydrazide side chain is able to stabilize the compounds in the binding site toward aspartic acid group present in the receptor through hydrogen bonding interactions. The X-ray crystal structures of compounds **7**-**10** has proven the existence of the compounds in the *cis* configuration, suggesting that the acid hyrazide group is essential in enhancing the potency of 2-furylbenzimidazoles as anti-angiogenic agents.

EXPERIMENTAL

Table 3. Summary of crystal data, data collection and refinement for the crystal structure determinations

Compound	**7**	**8**	**9**	**10**
Chemical formula	$C_{23}H_{24}N_4O_4S$	$C_{46}H_{44}N_8O_6$	$C_{22}H_{20}N_4O_2$	$C_{21}H_{18}N_4O_2$
Mol. Wt.	452.52	804.89	372.42	358.39
Color	Colorless	Colorless	Colorless	Yellow
Habit	Block	Needle	Fragment	Block
Crystal size (mm)	0.2×0.18×0.12	0.2×0.075×0.07	0.23×0.2×0.04	0.3×0.3×0.3
Lattice type	Monoclinic	Triclinic	Triclinic	Monoclinic
Space group	$P2_1/n$	P-1	P-1	$P2_1/c$
a (Å)	13.0995(6)	9.5576(3)	9.1823(7)	8.2328(3)
b (Å)	8.7233(4)	11.1611(4)	10.3588(7)	13.0220(4)
c (Å)	19.8027(9)	20.1377(7)	11.0190(9)	16.3746(5)
α (°)	90	88.6341(13)	106.962(5)	90
β (°)	93.666(2)	80.8042(13)	90.460(5)	90.2310(10)
γ (°)	90	76.9349(14)	107.525(5)	90
V (Å^3)	2258.24(18)	2065.49(12)	952.20(13)	1754.15(10)
Z	4	2	2	4
d_{cal} (Mg m^{-3})	1.331	1.294	1.299	1.357
Radiation	Cu Kα	Cu Kα	Cu Kα	Mo Kα
λ (Å)	1.54178	1.54178	1.54178	0.71073
μ (mm^{-1})	1.587	0.714	0.691	0.090
T (K)	100	100	100	100
θ_{max} (°)	68.483	68.489	66.7	36.514
Collec. Reflections	39617	41733	9336	80831
Indep. Reflections	4134	7545	3387	8609
R_{int}	0.0635	0.0391	0.0343	0.0239
Parameters	297	545	383	306
Restraints	0	2	160	34
S	1.008	1.063	1.070	1.043
R1 [I> 2σ(I)]	0.0412	0.0597	0.0657	0.0464
wR2 (all data)	0.1047	0.1539	0.2119	0.1439

All compounds were synthesized following procedures outlined by Temirak *et al.*[2] To a solution of the acid hyrazide (0.01 mol) in EtOH/AcOH (24:1, 25 mL), 0.02 mol of aryl aldehydes namely 4-methylbenzaldehyde, 4-methoxybenzaldehyde, and arylacetophenones namely acetophenone, 4-methylacetophenones, was added. The reaction mixture was heated under reflux for 5 h, and then cooled. The separated solids were filtered, dried, and re-crystallized from acetic acid to obtain pure product. Crystals suitable for X-ray diffraction for compound **7** and **10** were obtained by slow evaporation in DMSO and **8** and **9** were obtained from liquid diffusion from 1,4-dioxane/*n*-hexane. Diffraction data

for all compounds were collected on a Bruker APEX 2 DUO CCD diffractometer using graphite-monochromatted Mo-K_α (λ = 0.71073 Å) and Incoatec IμS Cu-K_α (λ = 1.54178 Å) radiation. Crystals were mounted on a MiTeGen MicroMount and collected at 100(2) K using an Oxford Cryosystems Cobra low temperature device.

Data was collected using omega and phi scans and were corrected for Lorentz and polarization effects using the APEX software suite.[22] Data were corrected for absorption effects using the multi-scan method (SADABS).[23] The structures were solved by direct methods and refined by full-matrix least-squares procedures on F^2 using SHELXL-2014 software.[24] All non-hydrogen atoms were refined anisotropically. Hydrogen atoms were added geometrically in calculated positions and refined using a riding model. Details of the data collection are given in Table 3. In structure **7** residual electron density surrounding S1s suggest a high degree of liberation movement in the solvent DMSO. In structure **8** the distance of N18 H18 and N18b H18b was restrained using (DFIX) Residual electron density around the 1,4-dioxane solvent molecule suggest a possible alternate conformation may be present. In structure **9** furan benzimidazole ring was modelled in two parts using restraints (DFIX, ISOR, RIGU) with an occupancy of 70, 30%. In structure **10** disorder in the furan ring was constrained and restrained using (EADP, SADI) and modelled over 3 positions with an occupancy of 56, 32 and 12%.

CCDC 1062711-1062714 contain the supplementary crystallographic data for this paper. These data can be obtained free of charge from The Cambridge Crystallographic Data Centre via www.ccdc.cam.ac.uk/data_request/cif.

ACKNOWLEDGEMENTS

This work was supported by a grant from Science Foundation Ireland (SFI IvP 13/IA/1894).

REFERENCES

1. S. Sato and S. Takenaka, Methods for Studying Nucleic Acid Drug Interactions, ed. by M. Wanunu and Y. Tor, CRC Press, New York, 2011, pp.111-112.
2. A. Temirak, Y. M. Shaker, F. A. F. Ragab, M. M. Ali., S. M. Soliman, J. Motier, G. Wolber, H. I. Ali, and H. I. El Diwani, *Arch. Pharm. Chem. Life Sci.*, 2014, 347, 291.
3. D. A. Horton, G. T. Bourne, and M. L. Smythe, *Chem. Rev.*, 2003, **103**, 893.
4. N. Perin, R. Nhili, K. Ester, W. Laine, G. Karminski-Zamola, M. Kralj, M.-H. David-Cordonnier, and M. Hranjec, *Eur. J. Med. Chem.*, 2014, **80**, 218.
5. C. Zimmer and U. Waehnert, *Prog. Biophys. Mol. Biol.*, 1986, **47**, 31.
6. Y. Kubota and H. Nakamura, *Chem. Lett.*, 1991, **5**, 745.

7. S. Nakano, N. Hasegawa, and Y. Kubota, *Nucl. Acids Symp. Ser*., 1994, **31**, 75.
8. J. Hackett, Z. Xiao, X. P. Zang, M. L. Lerner, D. J. Brackett, R. W. Brueggemeier, P. K. Li, and J. T. Pento, *Anticancer Res.*, 2007, **27**, 3801.
9. P. A. Renhowe, S. Pecchi, C. M. Shafer, T. D. Machajewski, E. M. Jazan, C. Taylor, W. Antonios-McCrea, C. M. McBride, K. Frazier, M. Wiesmann, G. R. Lapointe, P. H. Feucht, R. L. Warne, C. C. Heise, D. Menezes, K. Aardalen, H. Ye, M. He, V. Le, J. Vora, J. M. Jansen, M. E. Wernette-Hammond, and A. L. Harris, *J. Med. Chem.*, 2008, **52**, 278.
10. M. H. Pourgholami, Z. Y. Cai, S. Badar, K. Wangoo, M. S. Poruchynsky, and D. L. Morris, *BMC Cancer*, 2010, **10**, 143.
11. K. Li, T. M. Davis, C. Bailly, A. Kumar, D. W. Boykin, and W. D. Wilson, *Biochemistry*, 2001, **40**, 1150.
12. G. A. Ryzvanovich, R. S. Begunov, O. A. Rachinskaya, O. V. Muravenko, and A. A. Sokolov, *Pharm. Chem. J.*, 2011, **45**, 141.
13. P. D. Patel, M. R. Patel, N. Kaushik-Basu, and T. T. Talele, *J. Chem. Inf. Model.*, 2008, **48**, 42.
14. M. Hranjec, G. Pavlovic, and G. Karminski-Zamola, *Struct. Chem.*, 2007, **18**, 943.
15. D. K. Geiger, H. C. Geiger, and J. M. Deck, *Acta Cryst.*, 2014, **C70**, 1125.
16. K. T. Lin, J. C. Lien, C. H. Chung, S. C. Kuo, and T. F. Huang, *Eur. J. Pharmacol.*, 2010, **630**, 53.
17. H. L. Kuo, J. C. Lien, C. H. Chung, C. H. Chang, S. C. Lo, I. C. Tsai, H. C. Peng, S. C. Kuo, and T. F. Huang, *Naunyn Schmiedebergs Arch. Pharmacol*., 2010, **381**, 495.
18. S. W. Huang, J. C. Lien, S. C. Kuo, and T. F. Huang, *Carcinogenesis*, 2012, **33**, 1022.
19. A. Temirak, Y. M. Shaker, F. A.F. Ragab, M. M. Ali, H. I. Ali, and H. I. El Diwani *Eur. J. Med. Chem*., 2014, **87**, 868.
20. M. A. Omar, Y. M. Shaker, S. A. Galal, M. M. Ali, S. M. Kerwin, J. Li, H. Tokuda, R. A. Ramadan, and H. I. El Diwani, *Bioorg. Med. Chem*., 2012, **20**, 6989.
21. M. Cacic, M. Trkovnik, F. Cacic, and E. Has-Schon, *Molecules*, 2006, **11**, 134.
22. Bruker APEX v2014.11-0, Bruker AXS Inc., Madison, Wisconsin, USA.
23. SADABS (2014/5) Bruker AXS Inc., Madison, Wisconsin, USA; Sheldrick, G. M. University of Göttingen, Germany.
24. (a) SHELXL-2014, (2014), Bruker AXS Inc., Madison, Wisconsin, USA; Sheldrick, G. M. University of Göttingen, Germany; (b) G. M. Sheldrick, *Acta Cryst.*, 2015, **C71**, 3.